

BinConv: A Neural Architecture for Ordinal Encoding in Time-Series Forecasting

Andrei Chernov¹, Vitaliy Pozdnyakov², Ilya Makarov³

¹Independent Researcher; Germany

²AIRI, HSE University; Russia

³AIRI, ISP RAS, ITMO University; Russia

chernov.andrey.998@gmail.com, vvpozdnyakov@hse.ru, makarov@airi.net

Abstract

Recent work in time series forecasting has explored reformulating regression as a classification task. By discretizing the continuous target space into bins and predicting over a fixed set of classes, these approaches benefit from more stable training, improved uncertainty modeling, and compatibility with modern deep learning architectures. However, most existing methods rely on one-hot encoding, which ignores the inherent ordinal structure of the target values. As a result, they fail to convey information about the relative distance between predicted and true values during training. In this paper, we address this limitation by applying **Cumulative Binary Encoding** (CBE), a monotonic binary representation that transforms both model inputs and outputs. CBE implicitly preserves ordinal and magnitude information, allowing models to learn distance aware representations while operating within a classification framework. To leverage CBE effectively, we propose **BinConv**, a fully convolutional neural network architecture designed for probabilistic forecasting. We demonstrate that standard fully connected layers are not only less computationally efficient than convolutional layers when used with CBE, but also degrade forecasting performance. Our experiments on standard benchmark datasets show that BinConv achieves superior performance compared to widely used baselines in both point and probabilistic forecasting, while requiring fewer parameters and enabling faster training.

1 Introduction

Time series forecasting plays a key role in decision-making across domains such as finance (Akita et al. 2016), healthcare (Song et al. 2020), retail (Bandara et al. 2019), and climate science (Zaini et al. 2022). While classical methods like ARIMA and Exponential Smoothing remain widely used in practice (Hyndman and Athanasopoulos 2021), recent advances increasingly favor deep learning approaches (Lim and Zohren 2021; Li and Law 2024), particularly in scenarios requiring high-precision forecasting (Zhang et al. 2024).

A critical component of deep learning-based forecasting is data preprocessing. This typically includes normalization, min-max or mean scaling (Salinas et al. 2020), Box-Cox transformation (Hyndman and Athanasopoulos 2021), and short-time Fourier transforms (Furman et al. 2023). Recent studies (Ansari et al. 2024; Liu et al. 2024) have explored discretizing the continuous target space into fixed-size bins. Values are then represented as one-hot vectors, enabling a tokenized view of time series aligned with Transformer-style architectures. Empirical results suggest that such representations enhance performance, especially within Time Series Foundation Models (Zhang et al. 2024).

However, one-hot encoding lacks ordinal awareness,

treating bins as unrelated categories and ignoring relative distances, which are important for modeling temporal dynamics. To address this, we propose Cumulative Binary Encoding (CBE): a representation where all bins below (or equal to) the current value are activated. This monotonic encoding, previously applied to tabular data (Gorishniy, Rubachev, and Babenko 2022), preserves global ordinal structure and yields richer inputs for neural models.

Choosing an appropriate neural architecture is another central design decision. RNNs, CNNs, and Transformers are commonly used, with Transformer based models (Zhang et al. 2024) excelling due to their capacity for long range temporal modeling (Vaswani et al. 2017). Yet, their nearly quadratic complexity with sequence length (Tay et al. 2022) poses practical challenges.

As a result, in this paper we introduce **BinConv**, a CNN-based model that combines two dimensional and one dimensional convolutions to process CBE representations efficiently. Moreover, BinConv with CBE naturally supports probabilistic output by modeling distributions over bins, a capability often missing in standard CNN forecasting models. Remarkably, CBE and BinConv are effective only when used together. Our ablation study in Section 6 shows that neither CBE combined with a Transformer model nor one-hot encoding used with BinConv achieves satisfactory performance.

2 Related Work

Neural Network Architectures for Time Series Forecasting. Neural models vary in their trade-offs between accuracy, scalability, and speed. Transformer-based models such as PatchTST (Nie et al. 2023), TFT (Lim et al. 2021), and Informer (Zhou et al. 2021) capture long-range dependencies well, but incur high computational costs due to their quadratic scaling with sequence length. Earlier RNN-based models like LSTM (Hochreiter and Schmidhuber 1997), GRU (Che et al. 2018), and DeepAR (Salinas et al. 2020) are more efficient at inference, though limited by their sequential nature, which hinders training parallelism. CNN-based architectures such as TCN (Bai, Kolter, and Koltun 2018), DeepTCN (Chen et al. 2020), and ModernTCN (Luo and Wang 2024) offer fast, parallel training and strong forecasting performance. Following this line, our CNN-based BinConv model balances accuracy and efficiency when used with CBE inputs.

Token-Based Representations of Time Series. Inspired by NLP, recent work reformulates time series forecasting as next-token prediction using discretization. Models like LLMTTime (Gruver et al. 2023), TIMER (Liu et al. 2024), and Chronos (Ansari et al. 2024) encode values as digits, patches, or bins. Gorishniy et al. (Gorishniy, Rubachev, and

Babenko 2022) proposed piecewise linear encoding (PLE) for tabular data, preserving ordinal structure. Most models rely on one-hot encoding, which discards distance and order information between bins. This limits the ability to learn value relationships. In contrast, our CBE captures both order and magnitude, improving learning while remaining compatible with token-based models.

3 Cumulative Binary Encoding

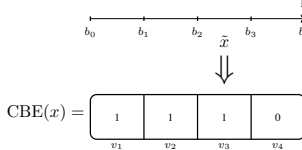


Figure 1: Example of CBE encoding for 4 bins.

The scale of time series can vary significantly, even within a single dataset. Therefore, before converting time series values into an encoding space, we apply normalization to map values into a quantized range. Similar to the Chronos model (Ansari et al. 2024), we use the mean scaling technique (Salinas et al. 2020), where each value is divided by the mean over a given context window. Specifically, we compute the scaled value as $\tilde{x} = x/s$, where $s = \frac{1}{C} \sum_{i=1}^C |x_i|$.

Next, we quantize the scaled time series as follows:

$$\begin{aligned} \text{CBE}(x) &= [v_1, \dots, v_D] \in \mathbb{R}^D \\ v_d &= \begin{cases} 0, & \tilde{x} < b_d \\ 1, & \tilde{x} \geq b_d \end{cases}, \end{aligned} \quad (1)$$

where b_d indicates a d -th bin in the original space. An example of construction of CBE is shown in Figure 1.

The interval from b_0 to b_D is uniformly split into D bins in a data-agnostic manner, where D , b_0 , and b_D are hyperparameters. In our experiments, we do not fine-tune these values per dataset and use fixed settings of $D = 1000$, $b_0 = -5$, and $b_D = 5$, unless stated otherwise. This quantization results in Cumulative Binary Encoding of the form 111...100...0.

This type of encoding is not new in the context of tabular deep learning for numerical features and can be viewed as a simplified version of the piecewise linear encoding proposed in (Gorishniy, Rubachev, and Babenko 2022). However, unlike previous work, we not only transform the inputs using this scheme, but also forecast targets directly in the encoding space, as detailed in Section 4.2. After generating a forecast in the encoding space, we apply an inverse transformation by assigning the average value of the bin encoding, i.e., $\hat{y} = (b_i + b_{i+1})/2$, where i is the index of the last 1. Finally, to obtain the forecast in the original space, we reverse the mean scaling: $y = s \cdot \hat{y}$. To the best of our knowledge, this approach is novel in the context of time series forecasting.

4 BinConv

4.1 Architecture

To model time series effectively in the discrete CBE space, the architecture must preserve ordinal relationships, support

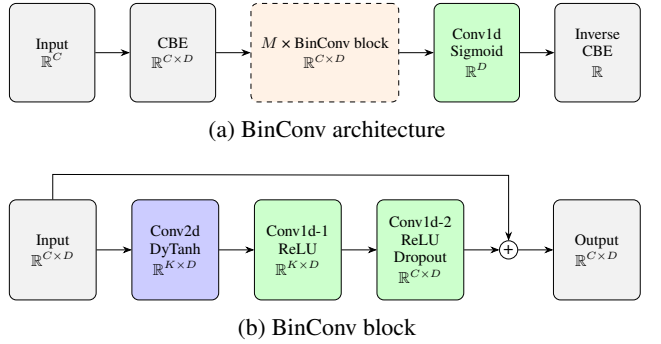


Figure 2: BinConv architecture. (a) First, we preprocess the time series using CBE. Then, the BinConv model is trained in the CBE space, and during forecasting, the inverse CBE transformation is applied to obtain predictions in the original space. BinConv consists of M stacked BinConv blocks followed by a final 1D convolution layer with a large kernel size. (b) Each BinConv block is the core component of the architecture, comprising three convolutional layers and a residual connection. The DyTanh activation function is used as a substitute for layer normalization. The output dimension of each BinConv block matches its input dimension.

Table 1: Convolutional parameters used in BinConv.

Layer	Kernel Size	In/Out Channels	Groups
Conv2d	(C, s_1)	$1 / K$	1
Conv1d-1	s_2	K / K	K
Conv1d-2	s_2	K / C	K
Conv1d	s_3	$C / 1$	1

autoregressive forecasting, and maintain computational efficiency. To this end, we propose BinConv, a convolutional neural architecture that efficiently captures the local temporal and monotonic structure of CBE vectors by combining 2D and 1D convolutions.

The BinConv model consists of M convolutional blocks followed by a final convolutional layer with a sigmoid activation function, producing an output vector in the CBE space (see Figure 2a). For each convolution, we add padding on both sides to preserve output dimensionality. To preserve the cumulative structure of the CBE representation, we use ones for left padding and zeros for right padding.

Each BinConv block comprises three convolutional layers (see Figure 2b). The first is a 2D convolution with kernel size $(C, 3)$, where C corresponds to the context length. This layer transforms the input matrix—obtained after applying CBE—into K one-dimensional vector representations, where K is the number of output channels and treated as a hyperparameter. Following the work of (Zhu et al. 2025), we use the DyTanh activation function, which replaces layer normalization in our architecture.

Next, we apply two 1D convolutional layers with ReLU activation, followed by dropout after the second layer. Inspired by (Liu et al. 2022; Luo and Wang 2024), we employ

depthwise convolution which is a special case of grouped convolution where the number of groups equals the number of channels K . This significantly reduces computational cost without sacrificing performance (see Section 6.4). Each BinConv block is designed such that the input and output dimensions are identical. This allows the use of a residual connection as the final operation in the block, enabling the stacking of multiple BinConv blocks while mitigating the vanishing gradient problem. The main parameters of the model are listed in Table 1.

To train the model, we apply the binary cross-entropy loss to the model output. This approach is analogous to a multi-label classification setup, where each class is predicted independently using a "one-versus-all" scheme.

4.2 Forecasting

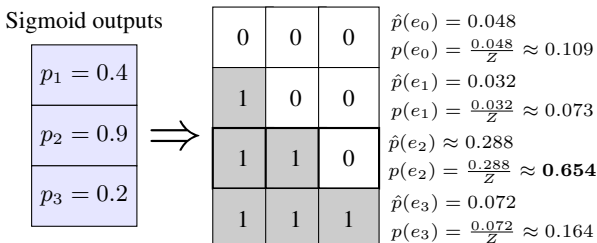
To forecast time series, we apply an autoregressive approach: forecasting at time step $t+1$, appending the result to the context, then forecasting at $t+2$, and so on. To do this, we need to transform the vector of sigmoid-activated outputs into a CBE. We interpret each component of the output as the success probability of an independent Bernoulli trial. Due to the design of the CBE, only sequences of the form $11\dots10\dots0$ are considered valid. Therefore, we normalize probability of each valid sequence by the total probability of all valid sequences, denoted as Z .

More formally, the probability of a valid encoding vector e_m , where the first m components are 1 and the remaining $D-m$ components are 0, is given by:

$$p(e_m) = \frac{\hat{p}(e_m)}{Z} = \frac{(\prod_{i=1}^m p_i) \left(\prod_{i=m+1}^D (1-p_i) \right)}{\sum_{j=0}^D \left(\prod_{i=1}^j p_i \prod_{i=j+1}^D (1-p_i) \right)}, \quad (2)$$

where p_i is the sigmoid output at position i .

Given these probabilities, we can either sample n trajectories autoregressively to obtain a probabilistic forecast, or take the argmax at each time step, which is faster but results in a point forecast. In Section 5, we show that the point estimates of the point and probabilistic forecasts do not differ significantly, and both outperform the point estimates of other models.



$$Z = \sum_m \hat{p}(e_m) = 0.048 + 0.032 + 0.288 + 0.072 = 0.44$$

Figure 3: Converting the neural network output $[0.4, 0.9, 0.2]$ into a CBE, the most probable sequence is $[1, 1, 0]$.

5 Experiments

5.1 Setup

We evaluate performance on three univariate datasets: M4 Daily (daily), M4 Weekly (weekly), and Tourism Monthly (tourism) (Makridakis, Spiliotis, and Assimakopoulos 2020; Athanasopoulos et al. 2011). The prediction horizon H for each dataset is set to 14, 13, and 24, respectively. The context length is set to $C = 3H$ for all datasets.

Additionally, we report long-term forecasting results on several multivariate datasets commonly used in the research community: ETTh1, ETTh2, ETTm1, ETTm2, and Illness (Zhang et al. 2024). The context length C and prediction horizon H were set to $C = H = 36$ for the Illness dataset and $C = H = 96$ for the others.

For the baseline models, we used the optimal hyperparameters provided in (Zhang et al. 2024). In contrast, BinConv was evaluated using its default configuration without any fine-tuning. This configuration is consistent across univariate and multivariate datasets, with the exception of the number of bins (see Table 2). For multivariate datasets, we reduced the number of bins to accelerate experiment runtime.

We adopt the training and evaluation setup from (Zhang et al. 2024). Specifically, we train each model for 50 epochs, and report evaluation metrics on the test set. For all models, we used the Adam optimizer (Kingma 2015) for training.

We evaluate point forecasts using the normalized mean absolute error (NMAE) and probabilistic forecasts using the continuous ranked probability score (CRPS), both widely adopted in time series forecasting research (Zhang et al. 2024; Chen et al. 2020; Ansari et al. 2024; Rasul et al. 2021b). The NMAE is defined as

$$\text{NMAE} = \frac{\sum_{k=1}^K \sum_{t=1}^T |x_t^k - \hat{x}_t^k|}{\sum_{k=1}^K \sum_{t=1}^T |x_t^k|},$$

where K is the dimensionality of the time series ($K = 1$ in the univariate case) and T is the prediction horizon. The CRPS is given by

$$\text{CRPS}(F^{-1}, x) = \int_0^1 2\Lambda_\alpha(F^{-1}(\alpha), x) d\alpha,$$

with quantile loss $\Lambda_\alpha(q, z) = (\alpha - \mathbb{I}\{z < q\})(z - q)$ and indicator function $\mathbb{I}\{\cdot\}$. We compute CRPS using 19 quantile levels and 100 samples to assess the quality of probabilistic forecasts, and NMAE to evaluate point forecasting performance following (Zhang et al. 2024).

For BinConv, as discussed in Section 3, we applied mean scaling independently to each sample prior to quantization. This was necessary because certain datasets, such as the M4 benchmark, consist of time series with widely varying scales.

All computations were performed on NVIDIA Tesla A10 GPU with 22.5 GB of RAM using CentOS 7 operating system, and all models were implemented using PyTorch 2.7.

5.2 Baseline Models

We select four representative baselines. First, we include PatchTST (Nie et al. 2023), a transformer based model that

achieves the best average performance across datasets in the ProbTS benchmark (Table 10 in (Zhang et al. 2024)). Second, we evaluate DLinear (Zeng et al. 2023), an efficient model in terms of both runtime and parameter count, while still achieving competitive performance.

Unlike BinConv, PatchTST and DLinear are non-autoregressive models: they predict the entire forecast horizon in a single inference pass. This design enables faster inference but lacks flexibility, as each change in forecast horizon requires retraining. In contrast, autoregressive models can adapt to arbitrary horizons at inference time. Additionally, PatchTST and DLinear are not probabilistic models and do not provide uncertainty estimates.

To address this gap in baselines, we include two autoregressive probabilistic models: GRU-NVP (Rasul et al. 2021b), which combines a GRU encoder with normalizing flows; and TimeGrad (Rasul et al. 2021a), which applies score based diffusion modeling to generate future trajectories by denoising noise conditioned on past observations.

For all four baselines, we adapt the hyperparameter configurations provided by the ProbTS benchmark.

We exclude foundation time series models from our baselines, as their zero shot performance remains inferior to that of state-of-the-art local models (Zhang et al. 2024; Toner et al. 2025).

5.3 Results

Table 2: Default hyperparameters used for BinConv. C denotes the context length. The only difference between univariate and multivariate setups is the number of bins.

Hyperparameter	Univariate	Multivariate
Number of bins (D)	1000	500
Minimum bin value (b_0)	-5	-5
Maximum bin value (b_D)	5	5
Number of channels (K)	C	C
K-size, conv-2D (s_1)	3	3
K-size, conv-1D (s_2)	3	3
K-size, final conv-1D (s_3)	51	51
Number of blocks (M)	3	3
Dropout	0.35	0.35
Learning rate	0.001	0.001

Univariate Datasets The comparison between models is presented in Table 3. We trained and evaluated all models using five different random seeds, and report the minimum, average, and maximum scores, as well as the standard deviation for each model. The results are summarized as follows:

- For every dataset and baseline, the average score is worse than the BinConv average score plus one standard deviation, indicating consistently better performance by BinConv.
- Except for the weekly dataset where TimeGrad achieves the best minimum score, BinConv outperforms all baselines in terms of minimum, average, and maximum scores across all datasets.

- For the CRPS metric, the improvement achieved by BinConv is statistically significant (p-value for T-test < 0.05) for all datasets and baselines, except TimeGrad on the weekly dataset.

- For the NMAE metric, the improvement is statistically significant (p-value for T-test < 0.05) for all datasets and baselines, except TimeGrad on the weekly dataset and DLinear on the daily dataset.

Additionally, Table 4 compares the performance of BinConv when using argmax-based versus sampling-based forecasting (see Section 4.2 for details). The results show that argmax-based forecasting does not degrade point forecasting performance.

Multivariate Datasets Due to the high computational cost, particularly for the TimeGrad model, which requires up to 20 hours for training and evaluation, we ran a single seed per model and multivariate dataset. Each dataset contains 7 variables. Since BinConv currently supports only univariate forecasting, and extending it to the multivariate setting is left for future work, we forecasted each time series independently using the sampling procedure described in Section 4.2.

In Table 5, we report CRPS and NMAE for all baseline models and BinConv. Since there is no consistent winner across all datasets, we additionally report average model rankings for both metrics. Rankings were computed based on relative performance: the best-performing model on each dataset was assigned rank 1, the second-best rank 2, and so on.

Remarkably, despite using untuned hyperparameters and not being explicitly designed for multivariate forecasting, BinConv achieved the best average rank based on the CRPS metric and the second-best rank based on the NMAE metric.

5.4 Efficiency of the Model

In Table 6, we report the total number of parameters for each model across all datasets. The DLinear model has significantly fewer parameters than the others, with BinConv being the second most parameter-efficient.

In Table 7, we present the average computation time during both training and inference for all models on the M4 Daily dataset. To obtain these results, we trained and evaluated all models using a batch size of 1, and computed the mean and standard deviation over all samples and epochs. As expected, DLinear is the fastest model during training, with BinConv being the second fastest.

During inference, PatchTST is the fastest model because it is non-autoregressive and predicts the entire forecast horizon in a single forward pass. DLinear ranks second, followed by BinConv and GRU-NVP, which exhibit similar inference speeds—approximately twice as slow as PatchTST. TimeGrad is significantly slower than all other models.

Using point (argmax-based) forecasting instead of sampling improves inference speed by approximately 25%. However, the difference is not dramatic, as sampling is implemented by duplicating the input N times, where N is the number of samples. This allows all N samples to be processed in a single batch.

Table 3: CRPS and NMAE results for all models. Each metric is reported as the average (avg), minimum (min), maximum (max), and standard deviation (std) over 5 different seeds. An asterisk (*) over the BinConv average score indicates that BinConv statistically significantly outperforms all baselines for that metric and dataset ($p < 0.05$).

Dataset	Stat	DLinear		PatchTST		GRU-NVP		TimeGrad		BinConv	
		CRPS	NMAE	CRPS	NMAE	CRPS	NMAE	CRPS	NMAE	CRPS	NMAE
daily	avg	0.0440	0.0440	<u>0.0438</u>	<u>0.0438</u>	0.0714	0.0782	0.0587	0.0696	0.0327*	0.0382
weekly	avg	0.1046	0.1046	<u>0.1039</u>	<u>0.1039</u>	<u>0.0972</u>	0.1062	0.1046	0.1283	0.0902	0.0972
tourism	avg	0.2745	0.2745	0.2633	<u>0.2633</u>	0.3723	0.4536	<u>0.2295</u>	0.2968	0.1824*	0.1955*
daily	min	<u>0.0394</u>	<u>0.0394</u>	0.0404	0.0404	0.0570	0.0649	0.0402	0.0475	0.0291	0.0341
weekly	min	0.1007	0.1007	0.1020	0.1020	0.0916	0.1034	0.0800	<u>0.0985</u>	<u>0.0851</u>	0.0921
tourism	min	0.2595	0.2595	0.2281	<u>0.2281</u>	0.2880	0.3849	<u>0.1993</u>	0.2596	0.1777	0.1911
daily	max	0.0506	0.0506	<u>0.0476</u>	<u>0.0476</u>	0.1196	0.1259	0.0933	0.1077	0.0366	0.0427
weekly	max	0.1072	<u>0.1072</u>	0.1078	0.1078	<u>0.1006</u>	0.1085	0.1718	0.2121	0.0981	0.1055
tourism	max	0.3077	0.3077	0.2888	<u>0.2888</u>	0.5799	0.5399	<u>0.2500</u>	0.3186	0.1892	0.2012
daily	std	0.0043	0.0043	0.0031	0.0031	0.0270	0.0266	0.0221	0.0252	<u>0.0037</u>	0.0043
weekly	std	<u>0.0025</u>	<u>0.0025</u>	0.0023	0.0023	0.0038	0.0026	0.0389	0.0488	<u>0.0050</u>	0.0052
tourism	std	0.0203	<u>0.0203</u>	0.0227	0.0227	0.1216	0.0696	<u>0.0200</u>	0.0235	0.0054	0.0049

Table 4: Comparison of BinConv performance using sampling versus argmax forecasting. Each metric is reported as the average (avg), minimum (min), maximum (max), and standard deviation (std) over 5 different seeds.

Dataset	Stat	Argmax		Sampling	
		CRPS	NMAE	CRPS	NMAE
daily	avg	0.037	0.037	0.033	0.038
weekly	avg	0.098	0.098	0.090	0.098
tourism	avg	0.196	0.196	0.182	0.196
daily	min	0.035	0.035	0.029	0.034
weekly	min	0.093	0.093	0.085	0.092
tourism	min	0.192	0.192	0.178	0.191
daily	max	0.039	0.039	0.037	0.044
weekly	max	0.105	0.105	0.098	0.106
tourism	max	0.201	0.201	0.189	0.201
daily	std	0.002	0.005	0.004	0.004
weekly	std	0.005	0.005	0.005	0.005
tourism	std	0.005	0.005	0.005	0.005

6 Ablation Study

6.1 Fully Connected Layers with BinConv

When designing the BinConv architecture, we intentionally excluded fully connected (FC) layers to maintain both strong generalization and parameter efficiency. Compared to convolutional layers, FC layers introduce significantly more trainable parameters, particularly problematic in high-dimensional output spaces. More critically, due to the design of CBE and the associated loss computation, an FC layer can restrict the model’s ability to forecast values beyond those observed during training. This limitation arises because FC layers lack weight sharing, meaning each output component is governed by an independent set of parameters. Conse-

quently, if the last K elements of a CBE target vector are frequently zero in the training set (a plausible scenario given that most targets are well below the maximum bin value b_D), the model may trivially learn to output zeros for these components. As a result, such an architecture fails to extrapolate to higher values during testing.

To illustrate this, we implemented a BinConv variant in which the final 1D convolution was replaced by an FC layer. The output of the BinConv blocks, $h \in \mathbb{R}^{C \times D}$, where C is the context length and D the number of bins, was averaged over the context dimension to yield $\bar{h} \in \mathbb{R}^D$, which was then mapped to \mathbb{R}^D via the FC layer. Using a synthetic dataset with a linear trend,

$$s_t = (100 + 1.5t)(1 + \sigma_t), \quad \sigma_t \sim \mathcal{N}(0, 10^{-4}),$$

We compared forecasts from the original BinConv and its FC-layer variant. While the original model successfully extrapolated the trend, the FC variant saturated at the maximum value seen during training, failing to capture future growth (Figure 4). To highlight this issue, we used per-dataset mean scaling on a synthetic example. Per-sample mean scaling partially mitigates the problem, as higher test-time values shift the mean, enabling some extrapolation.

Table 8 reports evaluation metrics for the FC variant with per-sample scaling (column “w/ FC Layer”). Despite reasonable results, the model cannot produce CBE vectors with more active bins than seen during training, as many neurons in the final layer become inactive and output constant values. In addition, as shown in Table 9, the FC layer significantly increases the number of parameters. Overall, the FC variant remains ill-suited for real-world forecasting tasks.

6.2 Transformer with CBE

An alternative to modifying only the final layer of BinConv is to replace the entire architecture with a transformer-based model, which relies exclusively on FC layers. However, our

Table 5: Forecasting performance (CRPS and NMAE) across different models and datasets. All datasets use context length 96 and prediction horizon 96 (except Illness, which uses 36 for both). Best scores per row are in bold. Bottom row shows average rank (lower is better).

Dataset	DLinear		PatchTST		GRU-NVP		TimeGrad		BinConv	
	CRPS	NMAE	CRPS	NMAE	CRPS	NMAE	CRPS	NMAE	CRPS	NMAE
ETTh1	0.3339	0.3339	0.3218	0.3218	0.3435	0.4383	0.2930	0.3867	0.2969	0.3201
ETTh2	0.2319	0.2319	0.1763	0.1763	0.2623	0.3100	0.2059	0.2574	0.1709	0.1853
ETTm1	0.2663	0.2663	0.2681	0.2681	0.4029	0.5018	0.4201	0.5153	0.2922	0.3141
ETTm2	0.1431	0.1431	0.1337	0.1337	0.2106	0.2618	0.1595	0.1930	0.1329	0.1456
Illness	0.1869	0.1869	0.1103	0.1103	0.0750	0.0828	0.0643	0.0868	0.1187	0.1447
Avg. Rank	3.4	2.8	2.4	1.8	4.2	4.0	2.8	3.8	2.2	2.6

Table 6: Total number of parameters (in thousands) per method and dataset.

Dataset	DLinear	BinConv	PatchTST	TimeGrad	GRU-NVP
daily	1.204	20.173	47.470	107.434	141.108
weekly	1.040	17.680	43.725	107.434	141.108
tourism	3.504	54.013	155.288	107.434	141.108

experiments show that this substitution results in a substantial performance drop. We evaluated both encoder-decoder and decoder-only transformer variants, and in all cases the results were unsatisfactory. For example, on the weekly dataset the NMAE increased by nearly an order of magnitude compared to BinConv, reaching values as high as 0.8 in the best-performing transformer configuration.

We attribute this degradation to the fundamental design of transformer architectures, which employ distinct weight matrices for processing each input component and generating each output component. While such flexibility is appropriate for one-hot encodings, it is ill-suited for the continuous bin encoding used in BinConv. As discussed in Section 6.1, CBE representations rarely contain vectors in which most components are exactly one or zero. This structural property favors architectures with weight sharing across components, ensuring that the model’s behavior is invariant to component position. Convolutional architectures naturally satisfy these constraints, making them more appropriate than transformers for processing CBE representations.

6.3 One-Hot Encoding with BinConv

In this section, we show that BinConv works poorly with one-hot encoding. We modify BinConv in a following way: we replace CBE with one-hot encoding both for input and output; replace final activation function from sigmoid to softmax and utilize standard multi-class cross entropy loss. For this variation NMAE on the weekly dataset increases from 0.09 to 1.18, which is notably worse than all other models and baselines considered in this study. The explanation of that is that BinConv architecture, as most convolution architectures, relies heavily on neighbours component, when it forecast the CBE is replaced with one-hot encoding, the convolutional network struggles to extract meaningful features because most of the receptive field is filled with zeros. This severely limits the network’s learning capacity, re-

sulting in significantly degraded performance. For example, NMAE on the weekly dataset increases from 0.09 to 1.18, which is notably worse than all other models and baselines considered in this study.

Unlike fully connected architectures such as transformers, BinConv operates over small local windows and therefore relies heavily on the relationships between neighboring components in the input encoding. This locality makes convolution particularly effective for structured encodings like CBE, where adjacent components often carry correlated information.

In contrast, for one-hot encodings, where exactly one component is equal to one and all others are zero, there is no meaningful local structure to exploit. The neighbors of the component with value one are always zero by design, making the surrounding values uninformative. In CBE, however, if a given component is equal to one, its neighboring components may still be either one or zero. For example, components to the right of a one-valued component may also be one, and components to the left of a zero-valued component may still be one. This structure enables convolutional filters to leverage informative local patterns, which is not possible with one-hot encodings.

6.4 Depthwise Convolution instead of Standard Convolution

Depthwise convolution is a form of convolution in which each input channel is convolved independently with its own filter. As a result, it requires significantly fewer convolutional kernels, which improves the model’s computational efficiency. In our model, we use this type of convolution in the BinConv block for 1D operations.

The performance of BinConv with standard 1D convolutional layers in place of depthwise layers is reported in Table 8, under the column labeled “w/SC”. Replacing depth-

Table 7: Mean and standard deviation of time (in seconds) to process a single sample for the M4 Daily dataset.

Phase	DLinear		BinConv		PatchTST		TimeGrad		GRU-NVP	
		Argmax		Sampling						
Train	0.0123 ± 0.0026	0.0284 ± 0.0043	0.0284 ± 0.0043		0.0381 ± 0.0049	0.0450 ± 0.0063	0.0362 ± 0.0048			
Inference	0.0755 ± 0.0016	0.09684 ± 0.00306	0.12788 ± 0.0017		0.0547 ± 0.0021	2.7723 ± 0.0365	0.1239 ± 0.0086			

Table 8: Comparison of architectural variants against the standard BinConv in terms of NMAE. The notation **w/** indicates that the standard BinConv is modified by replacing a specific component: **w/FC** uses a fully connected layer instead of the final convolution, **w/SC** replaces Depthwise convolutions with standard ones, colored arrows indicate whether a variant performs better (↓) or worse (↑) than BinConv.

Dataset	BinConv	w/FC	w/SC
daily	0.0382	0.0468 ↑	0.0343 ↓
weekly	0.0972	0.0943 ↓	0.1112 ↑
tourism	0.1955	0.1910 ↓	0.1945 ↓

Table 9: Number of parameters (in thousands) for the standard BinConv model and its architectural variations. See the caption of Table 8 for the explanation of the column notation.

Dataset	BinConv	w/FC	w/SC
daily	20.173	1019.540	51.679
weekly	17.680	1017.164	44.830
tourism	54.013	1052.210	146.899

wise convolutions with standard ones does not improve performance on any of the datasets, and it reduces model efficiency, as shown in Table 9.

7 Conclusion

In this paper, we proposed using Cumulative Binary Encoding (CBE) as a discrete quantization technique for time series, and we introduced BinConv, a convolutional architecture specifically designed for efficient processing of CBE vectors. Extensive evaluation on the publicly available ProbTS benchmark demonstrates that our method achieves state-of-the-art performance on univariate time series datasets and performs no worse on multivariate ones compared to strong baseline models. Through a comprehensive ablation study, we show that neither CBE with fully connected architectures nor BinConv with one-hot encoding performs nearly as well as the combination of CBE and BinConv.

Despite these promising results, our method has several limitations. First, CBE discretizes time series values, which requires approximating the precision of continuous data and can result in information loss. Second, selecting the number of bins introduces a trade-off: too few bins reduce representational fidelity, while too many increase computational

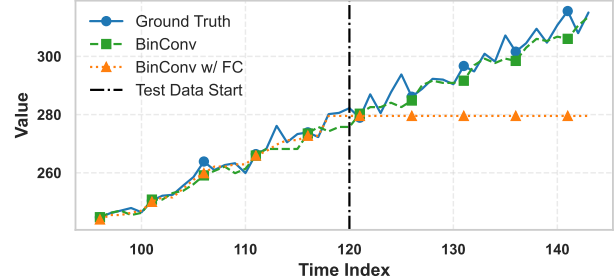


Figure 4: Forecast comparison of BinConv and BinConv w/ FC on synthetic linear trend data. The vertical line marks the start of the test data. BinConv w/ FC fails to forecast values beyond those seen during training.

complexity. Third, the current design is limited to univariate time series, which necessitates modeling each variable independently and prevents capturing cross-series interaction.

Future directions for this work include evaluating the generalization capability of our method in a Time Series Foundation Model setting, where the model is tested on previously unseen datasets. Another promising avenue is to extend the BinConv architecture to support multivariate time series by modeling interactions between components. Additionally, our approach could be applied to other time series tasks, such as imputation, anomaly detection, and classification.

References

Akita, R.; Yoshihara, A.; Matsubara, T.; and Uehara, K. 2016. Deep learning for stock prediction using numerical and textual information. In *2016 IEEE/ACIS 15th International Conference on Computer and Information Science (ICIS)*, 1–6. IEEE.

Ansari, A. F.; Stella, L.; Turkmen, A. C.; Zhang, X.; Mercado, P.; Shen, H.; Shchur, O.; Rangapuram, S. S.; Arango, S. P.; Kapoor, S.; Zschiegner, J.; Maddix, D. C.; Wang, H.; Mahoney, M. W.; Torkkola, K.; Wilson, A. G.; Bohlke-Schneider, M.; and Wang, B. 2024. Chronos: Learning the Language of Time Series. *Transactions on Machine Learning Research*. Expert Certification.

Athanasiopoulos, G.; Hyndman, R. J.; Song, H.; and Wu, D. C. 2011. The tourism forecasting competition. *International Journal of Forecasting*, 27(3): 822–844.

Bai, S.; Kolter, J. Z.; and Koltun, V. 2018. An empirical evaluation of generic convolutional and recurrent networks for sequence modeling. *arXiv preprint arXiv:1803.01271*.

Bandara, K.; Shi, P.; Bergmeir, C.; Hewamalage, H.; Tran, Q.; and Seaman, B. 2019. Sales demand forecast in e-commerce using a long short-term memory neural network methodology. In *Neural Information Processing: 26th International Conference, ICONIP 2019, Sydney, NSW, Australia, December 12–15, 2019, Proceedings, Part III* 26, 462–474. Springer.

Che, Z.; Purushotham, S.; Cho, K.; Sontag, D.; and Liu, Y. 2018. Recurrent neural networks for multivariate time series with missing values. *Scientific reports*, 8(1): 6085.

Chen, Y.; Kang, Y.; Chen, Y.; and Wang, Z. 2020. Probabilistic forecasting with temporal convolutional neural network. *Neurocomputing*, 399: 491–501.

Furman, Ł.; Duch, W.; Minati, L.; and Tolpa, K. 2023. Short-time Fourier transform and embedding method for recurrence quantification analysis of EEG time series. *The European Physical Journal Special Topics*, 232(1): 135–149.

Gorishniy, Y.; Rubachev, I.; and Babenko, A. 2022. On embeddings for numerical features in tabular deep learning. *Advances in Neural Information Processing Systems*, 35: 24991–25004.

Gruver, N.; Finzi, M.; Qiu, S.; and Wilson, A. G. 2023. Large language models are zero-shot time series forecasters. *Advances in Neural Information Processing Systems*, 36: 19622–19635.

Hochreiter, S.; and Schmidhuber, J. 1997. Long short-term memory. *Neural computation*, 9(8): 1735–1780.

Hyndman, R. J.; and Athanasopoulos, G. 2021. *Forecasting: principles and practice*. OTexts. OTexts: Melbourne, Australia. OTexts.com/fpp3. Accessed on May 2025.

Kingma, D. 2015. Adam: a method for stochastic optimization. *arXiv: 1412.6980*.

Li, W.; and Law, K. E. 2024. Deep learning models for time series forecasting: a review. *IEEE Access*.

Lim, B.; Arik, S. Ö.; Loeff, N.; and Pfister, T. 2021. Temporal fusion transformers for interpretable multi-horizon time series forecasting. *International Journal of Forecasting*, 37(4): 1748–1764.

Lim, B.; and Zohren, S. 2021. Time-series forecasting with deep learning: a survey. *Philosophical Transactions of the Royal Society A*, 379(2194): 20200209.

Liu, Y.; Zhang, H.; Li, C.; Huang, X.; Wang, J.; and Long, M. 2024. Timer: generative pre-trained transformers are large time series models. In *Proceedings of the 41st International Conference on Machine Learning*, 32369–32399.

Liu, Z.; Mao, H.; Wu, C.-Y.; Feichtenhofer, C.; Darrell, T.; and Xie, S. 2022. A convnet for the 2020s. In *Proceedings of the IEEE/CVF conference on computer vision and pattern recognition*, 11976–11986.

Luo, D.; and Wang, X. 2024. Moderntcn: A modern pure convolution structure for general time series analysis. In *The twelfth international conference on learning representations*, 1–43.

Makridakis, S.; Spiliotis, E.; and Assimakopoulos, V. 2020. The M4 Competition: 100,000 time series and 61 forecasting methods. *International Journal of Forecasting*, 36(1): 54–74.

Nie, Y.; Nguyen, N. H.; Sinhong, P.; and Kalagnanam, J. 2023. A Time Series is Worth 64 Words: Long-term Forecasting with Transformers. In *The Eleventh International Conference on Learning Representations*.

Rasul, K.; Seward, C.; Schuster, I.; and Vollgraf, R. 2021a. Autoregressive denoising diffusion models for multivariate probabilistic time series forecasting. In *International conference on machine learning*, 8857–8868. PMLR.

Rasul, K.; Sheikh, A.-S.; Schuster, I.; Bergmann, U. M.; and Vollgraf, R. 2021b. Multivariate Probabilistic Time Series Forecasting via Conditioned Normalizing Flows. In *International Conference on Learning Representations*.

Salinas, D.; Flunkert, V.; Gasthaus, J.; and Januschowski, T. 2020. DeepAR: Probabilistic forecasting with autoregressive recurrent networks. *International journal of forecasting*, 36(3): 1181–1191.

Song, Y.; Gao, S.; Li, Y.; Jia, L.; Li, Q.; and Pang, F. 2020. Distributed attention-based temporal convolutional network for remaining useful life prediction. *IEEE Internet of Things Journal*, 8(12): 9594–9602.

Tay, Y.; Dehghani, M.; Bahri, D.; and Metzler, D. 2022. Efficient transformers: A survey. *ACM Computing Surveys*, 55(6): 1–28.

Toner, W.; Lee, T. L.; Joosen, A.; Singh, R.; and Asenov, M. 2025. Performance of zero-shot time series foundation models on cloud data. *arXiv preprint arXiv:2502.12944*.

Vaswani, A.; Shazeer, N.; Parmar, N.; Uszkoreit, J.; Jones, L.; Gomez, A. N.; Kaiser, Ł.; and Polosukhin, I. 2017. Attention is all you need. *Advances in neural information processing systems*, 30.

Zaini, N.; Ean, L. W.; Ahmed, A. N.; and Malek, M. A. 2022. A systematic literature review of deep learning neural network for time series air quality forecasting. *Environmental Science and Pollution Research*, 1–33.

Zeng, A.; Chen, M.; Zhang, L.; and Xu, Q. 2023. Are transformers effective for time series forecasting? In *Proceedings of the AAAI conference on artificial intelligence*, volume 37, 11121–11128.

Zhang, J.; Wen, X.; Zhang, Z.; Zheng, S.; Li, J.; and Bian, J. 2024. ProbTS: Benchmarking point and distributional forecasting across diverse prediction horizons. *Advances in Neural Information Processing Systems*, 37: 48045–48082.

Zhou, H.; Zhang, S.; Peng, J.; Zhang, S.; Li, J.; Xiong, H.; and Zhang, W. 2021. Informer: Beyond Efficient Transformer for Long Sequence Time-Series Forecasting. In *The Thirty-Fifth AAAI Conference on Artificial Intelligence, AAAI 2021, Virtual Conference*, volume 35, 11106–11115. AAAI Press.

Zhu, J.; Chen, X.; He, K.; LeCun, Y.; and Liu, Z. 2025. Transformers without normalization. *arXiv preprint arXiv:2503.10622*.